Bridge Maintenance, Safety, Management, Digitalization and Sustainability – Jensen, Frangopol & Schmidt (eds)

Crowd-sensing drive-by monitoring for bridge frequency identification

Yifu Lan, Zhenkun Li & Weiwei Lin
Aalto University, Espoo, Finland

ABSTRACT: The drive-by inspection methods have garnered significant attention in recent years, owing to their advantages in mobility, cost-effectiveness, and efficiency. However, in practical applications, even simple extraction of bridge frequencies from an ordinary/commercial vehicle proves to be challenging; components associated with road roughness and vehicle dynamics typically dominate the vehicle vibration response. Current research typically attempts to alleviate these influences by minimizing variability (e.g., driving in the same lane, using the same speed, etc.), and by employing custom vehicles, though such practices are often difficult to implement. Recent advancements have pivoted towards "crowd-sensing" or "fleet monitoring" approaches, which undoubtedly introduce greater variability, thus potentially making the aforementioned strategies less preferable. In light of this, this paper presents a novel coherence-based approach applied to crowd-sensing drive-by monitoring systems which leverage data from multiple vehicles. The fundamental idea is to identify bridge frequencies as common vibrational components across a variety of vehicles driving over it. It encourages the introduction of variability in drive-by measurements to filter bridge frequencies. The proposed method is explored through numerical experiments, incorporating Monte Carlo methods. The results highlight the method's efficacy in eliminating the influences of road roughness, environmental noise, and vehicle parameter variations, with accurate identification of bridge frequencies. From the perspective of the method, this paper also illustrates the advantages of crowd-sensing drive-by monitoring and its practical feasibility in engineering problems.

1 INSTRUCTION

Bridge frequency plays a vital role in understanding essential characteristics of bridges (Nagayama et al. 2017). However, traditional methods of frequency measurement, which typically involve installing sensors directly on bridges, are fraught with challenges. These include substantial labor costs, risks related to onsite work, disruptions to traffic flow, and the expenses associated with sensor upkeep (Abdulkarem et al. 2020). An alternative is the drive-by method, which has seen a surge in interest and research activity recently. This technique utilizes vehicles as moving sensors, gathering dynamic data of bridges through the vehicle-bridge interaction (VBI) (Yang et al. 2004). It necessitates minimal equipment on the vehicle, presenting an effective and cost-efficient means of obtaining critical information about bridges (Lan et al. 2023, 2024).

However, in practice, even the seemingly simple task of extracting bridge frequencies can be quite challenging. Current research on drive-by monitoring mostly focuses on developing and validating methodologies in numerical studies, controlled laboratory environments, and small-scale structures using specialized vehicles (Malekjafarian et al. 2022). Drive-by measurements using ordinary/commercial vehicles on normal bridge structures are prone to large uncertainties (Nagayama et al. 2017). The amplitude of spectral peaks related to bridge frequencies may be low, and interference signals caused by road roughness components or

DOI: 10.1201/9781003483755-197

vehicle dynamics could mask the signals of interest. Non-bridge frequency peaks often combine with weak bridge frequency peaks (or are entirely absent), leading to misleading frequency identification (Lan et al. 2022). Therefore, discerning bridge information from the complex and variable signal components in vehicle responses is a key issue.

In light of this, considerable research has been conducted to eliminate the vibration components of the interference and extract the bridge frequency from the vehicle response. For instance, Yang et al. (2021) proposed to utilize the contact point (CP) response between the bridge and the vehicle to measure the bridge frequency; it was found to be independent of the vehicle frequency. This approach then removes the influence of surface irregularities by deducting the CP responses from two adjacent axles or trailers, allowing the bridge frequency to be deduced from the residual response. Nevertheless, practical implementation of such techniques often requires axles or trailers to follow identical trajectories and may necessitate the use of specialized vehicles or additional equipment like shakers (Yang et al. 2020, 2021, 2022). Unfortunately, these are not always available, and integrating such methods into commercial vehicles for daily monitoring proves even more challenging.

On the other hand, recent advancements have pivoted towards "crowd-sensing" or "fleet monitoring" approaches. Such methods can significantly reduce maintenance costs, as they do not require special arrangements for monitoring, including the custom vehicles (Mei & Gül 2019). Vibrational data of bridges can be automatically collected as vehicles pass over them, enabling the regular monitoring of numerous bridges within a region. Furthermore, due to its crowdsourcing nature, this technique offers robustness against operational effects and human errors. However, the crowd-sensing measurements will inevitably introduce greater variability (Mei et al. 2019; Mei & Gül 2019), potentially making the above strategies less desirable. There is a need to propose algorithms for crowd-sensing drive-by monitoring.

One idea is the application of cross-spectral estimation. Nagayama et al. (2017) utilized cross-spectral density function estimation techniques to extract bridge frequencies as common vibrational components in the responses of two ordinary vehicles. The effectiveness of this method was validated through field tests. Lan et al. (2023) obtained bridge frequencies as common signals among different sensors mounted on a truck model through laboratory experiments. In the cross-spectra obtained using these methods, peaks unrelated to the bridge frequencies were weakened. However, their performance is influenced by factors such as speed, road roughness, and vehicle weight; they are not always successful. In this regard, Lan et al. (2023) proposed a Coherence-PPI (Prominent Peak Identification) algorithm, a method that uses a Bayesian framework to further filter bridge-related peaks from a large number of coherences, allowing the identification of bridge frequencies under uncertainties such as road roughness. They verified the method by using multiple drive-by measurements of a city bus. The algorithm results demonstrate that more diverse vehicle parameters and more passing measurements are beneficial for filtering bridge frequencies. This also inspires the application of the algorithm to multi-vehicle tasks (i.e., crowd-sensing drive-by monitoring).

This study introduces a crowd-sensing drive-by monitoring algorithm for extracting bridge frequencies based on coherence and a Bayesian framework, which is a modification of the previously proposed Coherence-PPI algorithm by the authors. The underlying idea is to identify bridge frequencies as common vibrational components among different vehicles. Instead of using multiple runs of a single vehicle as input in previous studies, it utilizes runs by different vehicles as input (crowd-sensing measurements). To validate the proposed algorithm, a numerical study was conducted. The crowd-sensing measurements were simulated using vehicles with random parameters, and the effectiveness and robustness of them under various conditions (e.g., road roughness and environmental noise) were investigated using methods that include the Monte Carlo approach.

2 ALGORITHM

This algorithm is a revision of the previously proposed Coherence-PPI algorithm by the authors (Lan et al. 2023), modified for crowd-sensing measurements. It comprises three parts, namely coherence computation, threshold determination, and selection of prominent peaks

(PPs) and frequency identification. It is worth noting that some contents of the algorithm are simplified here. For a detailed description, one can refer to the original text.

2.1 *Coherence computation*

This step presents the methodology used for calculating coherence in crowd-sensing measurements. Generally, there are four main contributors to vehicle vibration: bridge vibration, road roughness, vehicle dynamics, and environmental noise. In the frequency spectrum, the peaks that correspond to bridge vibrations often appear less distinct in comparison to others. Yet, to some extent, they are deemed to exhibit a commonality across different passages. Peaks related to road roughness and vehicle dynamics tended to vary with different trajectory, speed, etc. Environmental noise is random. The coherence between the two signals is mathematically expressed as (Bendat & Piersol 2011):

$$C_{xy}(f) = \frac{\left|G_{xy}(f)\right|^2}{G_{xx}(f)G_{yy}(f)} \tag{1}$$

where $G_{xy}(f)$ is the cross-spectral density of signals x and y, $G_{xx}(f)$ is the power spectral density of signal x, and $G_{yy}(f)$ is the power spectral density of signal y.

For multi-vehicle passages on the same bridge, coherences are calculated for every possible pairing of them (see Figure 1). If there are n vehicle passages, then the total number of coherences is $N = C_n^2 = \frac{n(n-1)}{2}$. The coherence for any two runs, denoted as $\{X_i\}$, is computed using Equation 1. In this context, $\{X_i\}$ is a vector, and $[X]$ is a matrix consisting of N coherence vectors. It should be noted that due to varying speeds of different vehicles, their time-domain lengths differ. Thus, it is necessary to ensure that the input signals for algorithm are of equal length. In this regard, a 3-second time segment is selected from each signal to ensure they have equal frequency domain resolution.

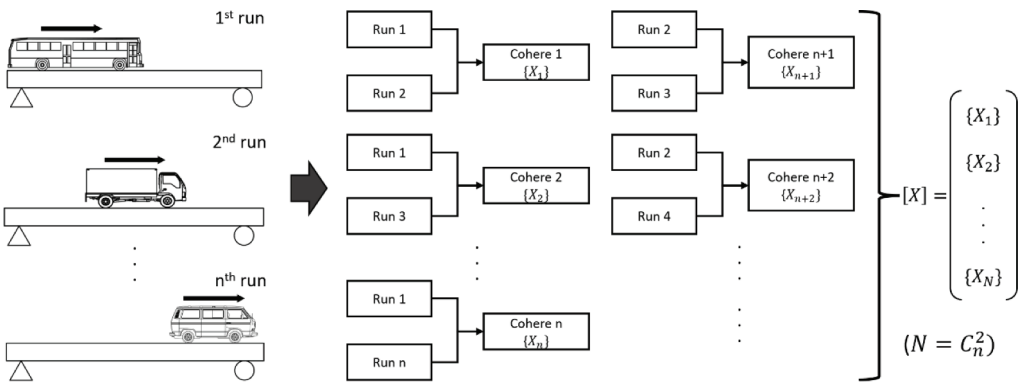

Figure 1. Coherence computation process.

2.2 *Threshold determination*

This step aims to determine the threshold that maximizes the occurrence of bridge-related frequencies. The Bayesian theorem (Bernardo & Smith 2009) provides a mathematical framework. Event B is defined as the attainment of the target frequency, and event H represents the occurrence when the coherence value is greater than or equal to a certain value (i.e., the threshold). The likelihood $P(H \mid B)$ signifies the probability that, when the target frequency is known, its corresponding coherence value is greater than the threshold. The prior $P(B)$ is the probability of attaining the target frequency in the absence of a threshold, whereas the evidence $P(H)$, is the probability that the coherence value is greater than the threshold. The

posterior $P(B \mid H)$, that is, the probability that the target frequency can be obtained when the threshold is given, can be calculated as:

$$P(B|H) = \frac{P(H|B) \cdot P(B)}{P(H)} \tag{2}$$

Building on earlier studies (Nagayama et al. 2017; Lan et al. 2023a, 2023b), bridge-related peaks are more likely to correspond to high percentile coherence values; that is, given the bridge frequency θ, it is more likely to correspond to a high percentile of coherence value t_0:

$$P[H(t_0)|B_\theta] > E(P) \tag{3}$$

The distribution of all coherence values may approximate a normal distribution. Considering that $P(B)$ is a constant, it suggests that choosing a larger threshold value for coherence is reasonable (Lan et al. 2023).

According to the 3-sigma rule in statistics, in a normal distribution, approximately 68% of observations fall within one standard deviation of the mean ($\tau = 0.84$), 95% within two standard deviations ($\tau = 0.975$), and 99.7% within three standard deviations ($\tau = 0.9985$). In this study, a threshold of $\tau = 0.84$ can be chosen.

2.3 *Selection of PPs and frequency identification*

This step counts the probability of each frequency interval above the threshold. The frequency range from 0 to 50Hz is divided into 100 intervals (θ_1,θ_2...,θ_{100}), with each representing a 0.5Hz interval. The interval, θ, containing the bridge frequency will exhibit the maximum probability value. During the procedure, the peaks in coherence that exceed the threshold, denoted as P_i, along with their corresponding frequencies F_i, are recorded. They are used to form a new matrix, [P], which can be thought of as a prominent peak matrix:

$$\begin{bmatrix} P_1 P_2 \dots P_n \\ F_1\ F_2 \dots F_n \end{bmatrix} = [P] \tag{4}$$

Then, the occurrence of these prominent peaks (PP) within each frequency interval is counted. The interval of the maximum occurrences is indicative of the bridge's fundamental frequency.

3 VBI MODEL

To validate the algorithm and to study the impact of various factors, a numerical study will be conducted. The following presents the construction of the VBI model used for the simulations in this work. A 2-DOF quarter-car model is utilized to simulate the rear axle system of a vehicle, and at the same time, an Euler-Bernoulli beam model is used to represent the simply supported bridge, as shown in Figure 2. This simplification aligns with that used in the study by Liu et al. (2023), who demonstrated that overlooking the impact of front suspension vibrations on the rear axle system is akin to introducing a certain level of noise into the results, which they deemed acceptable. This study adopts an unusually high noise level (10%), contrasting with previous studies that often considered 5% as a high noise level (Li et al. 2023). The adoption of the 2-DOF quarter-car model offers a compromise between model complexity and computational efficiency. This is particularly beneficial for implementing computationally intensive methods such as Monte Carlo simulations. For the bridge, each node in this finite element (FE) beam model is characterized by 2 DOFs: vertical translation and rotation. The beam model comprises n elements and $n + 1$ nodes, resulting in a total of $2n$ DOFs, not including the vertical constraints at the ends of the bridge. The bridge has a total length of L, and it features uniform flexural rigidity, denoted as EI, and a consistent mass per unit length, represented by m. Additionally, the damping characteristics of the bridge are approximated using mass-stiffness proportional Rayleigh damping.

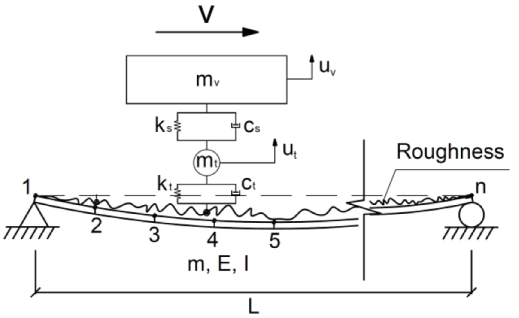

Figure 2. VBI model.

The fundamental equations governing the VBI system are as follows:

$$[M_v]\{\ddot{y}_v\} + [C_v]\{\dot{y}_v\} + [K_v]\{y_v\} = \{F_{cv}\} \tag{5}$$

$$[M_b]\{\ddot{y}_b\} + [C_b]\{\dot{y}_b\} + [K_b]\{y_b\} = \{F_{cb}\} \tag{6}$$

For the vehicle, $[M_v]$, $[C_v]$, and $[K_v]$ signify the vehicle's mass, damping, and stiffness matrices, respectively, and $\{y_v\}$ is the displacement vector. The time-varying interaction force on the vehicle is $\{F_{cv}\}$. For the bridge, $[M_b]$, $[C_b]$, and $[K_b]$ denote the bridge's mass, damping, and stiffness matrices, respectively, and $\{y_b\}$ is the bridge's nodal displacement vector. The force acting on the bridge is represented by $\{F_{cb}\}$.

The subsystem matrices and response vector for the vehicle model are as follows, where the body and axle masses are denoted by m_v and m_t, the suspension and tire damping by c_s and c_t, and the suspension and tire stiffness by k_s and k_t, respectively. The vertical displacements of the vehicle body and axle are denoted u_v and u_t, respectively.

$$[M_v] = \begin{bmatrix} m_v & \\ & m_t \end{bmatrix} \tag{7}$$

$$[C_v] = \begin{bmatrix} c_s & -c_s \\ -c_s & c_s + c_t \end{bmatrix} \tag{8}$$

$$[K_v] = \begin{bmatrix} k_s & -k_s \\ -k_s & k_s + k_t \end{bmatrix} \tag{9}$$

$$\{y_v\} = \begin{bmatrix} u_v & u_t \end{bmatrix}^T \tag{10}$$

The Newmark-Beta method is used to obtain the dynamic responses of the vehicle through the VBI process. The parameters β and γ of the Newmark-Beta method are selected as 0.25 and 0.5, respectively.

In this study, road roughness is simulated according to ISO 8608 (Múčka 2018), using a Power Spectral Density (PSD) function that characterizes roughness for different classes. Five roughness classes are defined, with coefficients: Class A ($0 - 2^5$), B ($2^5 - 2^7$), C ($2^7 - 2^9$), D ($2^9 - 2^{11}$), and E ($2^{11} - 2^{13}$) in units of $10^{-6}m^3$. A standard zero-mean real-valued stationary Gaussian process simulates the surface roughness profile, summing harmonic waves with specific spatial frequencies and random phase angles to construct the profile.

This noise is introduced into the signal using the formula given in Equation 11 (Xu et al. 2022). In this equation, $\ddot{u}_p$ represents the acceleration data of the vehicle that has been polluted. The term E_p denotes the level of environmental noise, N_s is a variable following the standard normal distribution, and $\sigma_{\ddot{u}_v}$is the standard deviation of the vehicle's acceleration response, denoted by $\ddot{u}_v$. In this study, noise is set to be 10%.

$$\ddot{u}_p = \ddot{u}_v + E_p N_s \sigma_{\ddot{u}_v} \tag{11}$$

4 NUMERICAL STUDY

4.1 *Simulations and algorithm results*

In this section, the simulation of crowd-sensing measurements over a bridge will be demonstrated using vehicles with random parameters. The bridge parameters are: m = 2000 kg/m, $EI = 6.06 \times 10^{1\circ}$ N·m^2, L = 45 m. The random parameters will be selected within a normal distribution based on the rear axle parameters of a bus. For example, the parameters of a bus can be: $m_v = 1.0 \times 10^4$ kg, $m_t = 1.0 \times 10^3$ kg, $c_s = 1.0 \times 10^4$ N·s/m, $c_t = 0$, $k_s = 4.0 \times 10^5$ N/m, $k_t = 3.5 \times 10^6$ N/m, and v = 7.5 m/s. The randomly generated vehicle parameters for the $i-th$ passage can be represented as follows:

$$Para_i^* = normrnd(Para, \sigma) \tag{12}$$

where *normrnd* is the normal distribution function, *Para* denotes the baseline bus parameters, which is the above-mentioned m_v, c_s, etc., and σ is the standard deviation of the normal distribution. In this study, it is taken as one-quarter of the original parameter (i.e., *Para*/4).

Under Grade "E" road conditions (poorest), it is evident from the responses obtained using vehicles with baseline parameters (see Figure 3a) that, although some peaks in the spectrum appear to be related to the bridge frequency, it is challenging to determine the bridge frequency. By contrast, in the algorithm results obtained from 100 random vehicle measurements (see Figure 3b), the bridge frequency can be clearly identified as the most prominent peak even under the poorest road roughness. Measurements obtained from multiple vehicles can filter the bridge-related components in the signal, because the distinct characteristics of each vehicle infuse variability into the non-bridge components of the signals. This proves the effectiveness of the proposed algorithm. It is noteworthy that this work only considered the scenario of a single vehicle on the bridge at a time. The case of multiple vehicles simultaneously on the bridge merits further exploration in future research.

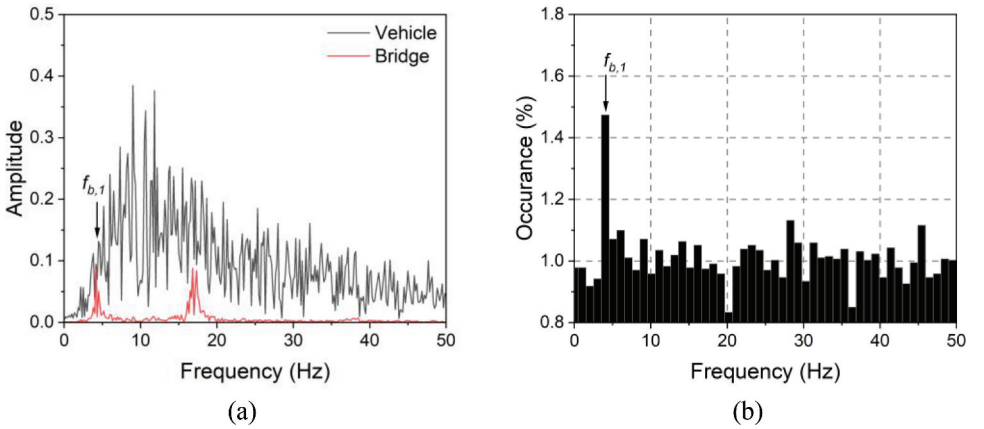

Figure 3. Frequency identification results: (a) frequency spectrum; (b) algorithm output.

4.2 *Effect of vehicle runs and Monte Carlo simulations*

This study also explored the effect of the number of vehicle passages on the results. Under the same conditions and using random functions as above, the algorithm results for different vehicle passages are illustrated in Figure 4. When results are obtained from a smaller number of vehicle passes, the peaks associated with the bridge frequency may not be well identified. Therefore, an adequate number of runs should be ensured to achieve statistical significance in the results; in this study, 50 passages were found to be sufficient.

This section also employs Monte Carlo simulations to validate the robustness of the proposed algorithm. The fundamental concept of Monte Carlo simulations is to utilize randomness to solve problems that could, in principle, be deterministic (Z.Mooney 1997). Utilizing

VBI simulations, random samples are produced, where each set of 50 samples (equating to 50 vehicle passages) is used as a single algorithm input, denoted as $[X]q$ (q=1, 2, 3…), with the corresponding output being $P_q(B_\theta \mid H_\tau)$. When the algorithm is run 2000 times for each road roughness, the Monte Carlo result for that roughness level should be $\frac{1}{2000}\sum_{q=1}^{2000} P_q(B_\theta \mid H_\tau)$. From Figure 5, it is evident that the algorithm performs effectively and similarly across various road roughness. This demonstrates the robustness of the proposed algorithm and its insensitivity to road surface conditions, which is considered one of the most critical factors affecting drive-by methods.

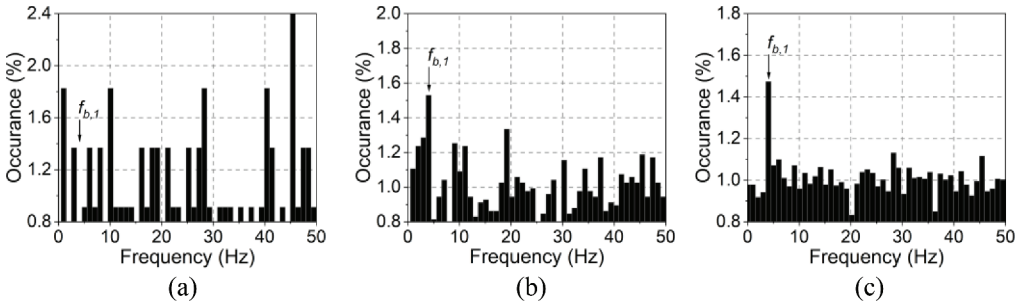

Figure 4. Algorithm outputs for different vehicle runs: (a) runs = 10; (b) runs = 50; (c) runs = 100.

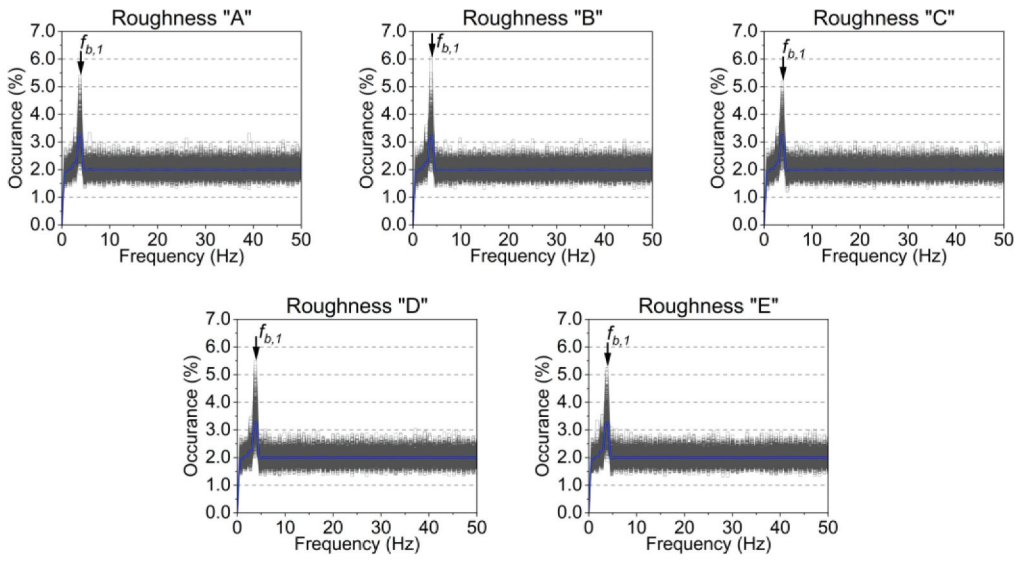

Figure 5. Monte Carlo results.

5 CONCLUSION

This study presents a crowd-sensing drive-by monitoring algorithm for extracting bridge frequencies. It is a modification of the Coherence-PPI algorithm previously proposed by the authors, adapted for multi-vehicle measurements. To validate the proposed algorithm, a numerical study was conducted, where the crowd-sensing measurements were simulated using vehicles with random parameters. According to numerical studies, several conclusions can be drawn:

(1) Under the influence of road roughness and environmental noise, the algorithm based on crowd-sensing measurements successfully identifies the bridge's fundamental frequency.

(2) The frequencies identified by the algorithm are statistical results, where numerous measurements enhance clarity and ensure reliability in frequency estimation.
(3) The robustness of this method has been examined using the Monte Carlo approach. The algorithm's outcomes are unaffected by the level of road roughness.

Despite the findings summarized above, field tests are required to assess the performance of this method in practice.

ACKNOWLEDGMENT

This research is sponsored by the Jane and Aatos Erkko Foundation in Finland (Grant No. 210018). Any findings, opinions, conclusions, and recommendations of this paper are those of the authors and do not necessarily reflect the views of the research sponsor.

REFERENCES

Nagayama, T., Reksowardojo, A.P., Su, D. & Mizutani, T.2017. Bridge natural frequency estimation by extracting the common vibration component from the responses of two vehicles. *Engineering Structures* 150: 821–829.

Abdulkarem, M., Samsudin, K., Rokhani, F.Z. & A Rasid, M.F. 2020. Wireless sensor network for structural health monitoring: A contemporary review of technologies, challenges, and future direction. *Structural Health Monitoring* 19(3): 693–735.

Yang, Y.B., Lin, C.W. & Yau, J.D. 2004. Extracting bridge frequencies from the dynamic response of a passing vehicle. *Journal of Sound and Vibration* 272(3): 471–493.

Lan, Y., Zhang, Y. & Lin, W. 2023. Diagnosis algorithms for indirect bridge health monitoring via an optimized AdaBoost-linear SVM. *Engineering Structures* 275: 115239.

Lan, Y., Li, Z. & Lin, W. 2024. Physics-guided diagnosis framework for bridge health monitoring using raw vehicle accelerations. *Mechanical Systems and Signal Processing* 206: 110899.

Malekjafarian, A., Corbally, R. & Gong, W. 2022. A review of mobile sensing of bridges using moving vehicles: Progress to date, challenges and future trends. *Structures* 44: 1466–1489.

Lan, Y., Lin, W. & Zhang, Y. 2022. Bridge frequency identification using vibration responses from sensors on a passing vehicle. *Bridge Safety, Maintenance, Management, Life-Cycle, Resilience and Sustainability*. CRC Press.

Yang, Y.B., Mo, X.Q., Shi, K., Wang, Z.L., Xu, H. & Wu, Y.T. 2021. Contact Residue for Simultaneous Removal of Vehicle's Frequency and Surface Roughness in Scanning Bridge Frequencies Using Two Connected Vehicles. *International Journal of Structural Stability and Dynamics* 21(13): 2171006.

Yang, Y.B., Xu, H., Zhang, B., Xiong, F. & Wang, Z.L. 2020. Measuring bridge frequencies by a test vehicle in non-moving and moving states. *Engineering Structures* 203: 109859.

Yang, Y.B., Huang, C.C., Xu, H., Wang, M.H., Wang, Z.L. & Shi, K. 2022. Frequency extraction for bridges with rough surface by a moving test vehicle enhanced by a shaker. *Engineering Structures* 266: 114598.

Mei, Q. & Gül, M. 2019. A crowdsourcing-based methodology using smartphones for bridge health monitoring. *Structural Health Monitoring* 18(5–6): 1602–1619.

Mei, Q., Gül, M. & Boay, M. 2019. Indirect health monitoring of bridges using Mel-frequency cepstral coefficients and principal component analysis. *Mechanical Systems and Signal Processing* 119: 523–546.

Lan, Y., Lin, W. & Zhang, Y. 2023. Bridge Frequency Identification Using Multiple Sensor Responses of an Ordinary Vehicle. *International Journal of Structural Stability and Dynamics* 23(05): 2350056.

Lan, Y., Li, Z., Koski, K., Fülöp, L., Tirkkonen, T. & Lin, W. 2023. Bridge frequency identification in city bus monitoring: A coherence-PPI algorithm. *Engineering Structures* 296: 116913.

Bendat, J.S. & Piersol, A.G. 2011. *Random data: analysis and measurement procedures*. John Wiley & Sons.

Bernardo, J.M. & Smith, A.F. 2009. *Bayesian theory*. John Wiley & Sons.

Liu, C., Zhu, Y. & Ye, H. 2023. Bridge frequency identification based on relative displacement of axle and contact point using tire pressure monitoring. *Mechanical Systems and Signal Processing* 183: 109613.

Li, Z., Lan, Y. & Lin, W. 2023. Indirect damage detection for bridges using sensing and temporarily parked vehicles. *Engineering Structures* 291: 116459.

Múčka, P. 2018. Simulated Road Profiles According to ISO 8608 in Vibration Analysis. *Journal of Testing and Evaluation* 46: 20160265.

Xu, H., Liu, Y.H., Wang, Z.L., Shi, K., Zhang, B. & Yang, Y.B. 2022. General contact response of single-axle two-mass test vehicles for scanning bridge frequencies considering suspension effect. *Engineering Structures* 270: 114880.

Z.Mooney, C. 1997. *Monte Carlo Simulation*. SAGE Publications, Inc.